

This is a repository copy of *Complement receptor 1 is the human erythrocyte receptor for Plasmodium vivax erythrocyte binding protein.*

White Rose Research Online URL for this paper:

<https://eprints.whiterose.ac.uk/id/eprint/209360/>

Version: Published Version

Article:

Lee, Seong-Kyun, Crosnier, Cécile orcid.org/0000-0003-0619-9797, Valenzuela-Leon, Paola Carolina et al. (7 more authors) (2024) Complement receptor 1 is the human erythrocyte receptor for Plasmodium vivax erythrocyte binding protein. Proceedings of the National Academy of Sciences of the United States of America. e2316304121. ISSN: 1091-6490

<https://doi.org/10.1073/pnas.2316304121>

Reuse

This article is distributed under the terms of the Creative Commons Attribution-NonCommercial-NoDerivs (CC BY-NC-ND) licence. This licence only allows you to download this work and share it with others as long as you credit the authors, but you can't change the article in any way or use it commercially. More information and the full terms of the licence here: <https://creativecommons.org/licenses/>

Takedown

If you consider content in White Rose Research Online to be in breach of UK law, please notify us by emailing eprints@whiterose.ac.uk including the URL of the record and the reason for the withdrawal request.



Complement receptor 1 is the human erythrocyte receptor for *Plasmodium vivax* erythrocyte binding protein

Seong-Kyun Lee^a, Cécile Crosnier^b, Paola Carolina Valenzuela-Leon^a , Brian L. P. Dizon^{c,d}, John P. Atkinson^e , Jianbing Mu^a, Gavin J. Wright^b, Eric Calvo^a , Karthigayan Gunalan^{a,1}, and Louis H. Miller^{a,1}

Contributed by Louis H. Miller; received September 19, 2023; accepted December 20, 2023; reviewed by Didier Ménard and Wai-Hong Tham

The discovery that Africans were resistant to infection by *Plasmodium vivax* (*P. vivax*) led to the conclusion that *P. vivax* invasion relied on the *P. vivax* Duffy Binding Protein (PvDBP) interacting with the Duffy Antigen Receptor for Chemokines (DARC) expressed on erythrocytes. However, the recent reporting of *P. vivax* infections in DARC-negative Africans suggests that the parasite might use an alternate invasion pathway to infect DARC-negative reticulocytes. To identify the parasite ligands and erythrocyte receptors that enable *P. vivax* invasion of both DARC-positive and -negative erythrocytes, we expressed region II containing the Duffy Binding-Like (DBL) domain of *P. vivax* erythrocyte binding protein (PvEBP-RII) and verified that the DBL domain binds to both DARC-positive and -negative erythrocytes. Furthermore, an AVIDITY-based EXtracellular Interaction Screening (AVEXIS) was used to identify the receptor for PvEBP among over 750 human cell surface receptor proteins, and this approach identified only Complement Receptor 1 (CR1, CD35, or C3b/C4b receptor) as a PvEBP receptor. CR1 is a well-known receptor for *P. falciparum* Reticulocyte binding protein Homology 4 (PfRh4) and is present on the surfaces of both reticulocytes and normocytes, but its expression decreases as erythrocytes age. Indeed, PvEBP-RII bound to a subpopulation of both reticulocytes and normocytes, and this binding was blocked by the addition of soluble CR1 recombinant protein, indicating that CR1 is the receptor of PvEBP. In addition, we found that the Long Homology Repeat A (LHR-A) subdomain of CR1 is the only subdomain responsible for mediating the interaction with PvEBP-RII.

Plasmodium vivax | erythrocyte binding protein | complement receptor 1

Plasmodium vivax is the most widespread species of malaria-causing parasites outside of Africa, but the exact frequency in Africa remains unknown (1). It is known that *P. vivax* merozoites exclusively invade reticulocytes from Duffy Antigen Receptor for Chemokine (DARC) positive individuals through a well-known interaction between *P. vivax* Duffy Binding Protein (PvDBP) and DARC (2, 3). However, the increasing reports of *P. vivax* infections in DARC-negative people in many parts of Africa (4) imply that invasion is also accomplished through other host and parasite molecules along with the PvDBP–DARC interaction. For example, *P. vivax* Reticulocyte Binding Protein 2b (PvRBP2b) was identified as binding to a reticulocyte-specific receptor, transferrin receptor 1 (TfR1 or CD71) (5, 6), and later PvRBP2a was identified to bind to CD98 (7). In addition, several ligands have been shown to bind to erythrocytes such as the *P. vivax* Merozoite Surface Protein 1 paralog (PvMSP1P) (8, 9), the GPI-Anchored Micronemal Antigen (PvGAMA) (10–12), the Reticulocyte Binding Proteins (PvRBPs) (5, 7), the Tryptophan Rich Antigen (PvTRAg) family (13), and the Erythrocyte Binding Protein Region II (PvEBP-RII) (14, 15). Among these ligands, however, only a few have been found to be able to bind erythrocytes from DARC-negative individuals, and PvEBP is one of these ligands (14). The *pvebp* gene is not present in the monkey-adapted *P. vivax* strain (Salvador-1) but was first identified in the *P. vivax* genome from a Cambodian field isolate (16). Interestingly, in a later study, more copies of *pvebp* gene were identified in isolates from Madagascar where both DARC-positive and -negative individuals coexist compared to Cambodia (17) suggesting that PvEBP may play a role in DARC-negative infection. Indeed, in our previous study, PvEBP-RII showed binding activity to erythrocytes from both DARC-positive and -negative individuals using a COS7 cell binding assay, albeit with smaller rosette number and size compared to the regions II of PvDBP (PvDBP-RII) (14). In another study, PvEBP-RII recombinant protein that is expressed in bacteria did not demonstrate binding to DARC-negative erythrocytes (15). In our present study, we reconfirmed the binding activity of recombinant PvEBP-RII expressed in mammalian cells not only to reticulocytes but also to normocytes from both DARC-positive and -negative individuals.

Significance

Elucidating the molecular basis of erythrocyte invasion by *Plasmodium* parasites is a rational way of identifying parasite ligands and erythrocyte receptors involved in invasion and reveals promising candidates for antimalarial vaccines. This study identifies the erythrocyte receptor for the *P. vivax* erythrocyte binding protein (PvEBP), part of the family that includes the Duffy Binding Protein (DBP). The PvEBP binds erythrocyte Complement Receptor 1 (CR1) regardless of Duffy Antigen Receptor for Chemokine's (DARC) presence on erythrocytes. While DBP has been studied as a vaccine candidate for *P. vivax*, its effectiveness may be limited in regions where the DARC is reduced like in Africa. Thus, EBP together with DBP may offer a more viable vaccine option for African *P. vivax* parasites.

Author contributions: K.G. and L.H.M. designed research; S.-K.L., C.C., P.C.V.-L., and J.M. performed research; J.P.A., G.J.W., and E.C. contributed new reagents/analytic tools; S.-K.L., C.C., B.L.P.D., G.J.W., and K.G. analyzed data; and S.-K.L., K.G., and L.H.M. wrote the paper.

Reviewers: D.M., Institut Pasteur; and W.-H.T., Walter and Eliza Hall Institute of Medical Research.

The authors declare no competing interest.

Copyright © 2024 the Author(s). Published by PNAS. This article is distributed under [Creative Commons Attribution-NonCommercial-NoDerivatives License 4.0 \(CC BY-NC-ND\)](#).

¹To whom correspondence may be addressed. Email: Karthigayan.gunalan@nih.gov or lmiller@niaid.nih.gov.

This article contains supporting information online at <https://www.pnas.org/lookup/suppl/doi:10.1073/pnas.2316304121/-DCSupplemental>.

Published January 23, 2024.

To identify potential host receptors for PvEBP, we systematically tested recombinant PvEBP-RII for direct binding to the entire ectodomains of over 750 human surface receptor proteins using AVIDity-based EXtracellular Interaction Screen (AVEXIS) (18–21). This approach has been used to identify low-affinity protein–protein interactions by the purposeful oligomerization of a soluble enzyme-linked parasite ligand and systematic testing for direct binding to an array of human receptor ectodomains. Using the AVEXIS approach, we observed that PvEBP-RII binds to Complement Receptor 1 (CR1, CD35, or C3b/C4b receptor), a receptor protein known to be expressed on the erythrocytes and responsible for the Knops blood group system (22, 23). CR1 is a well-known receptor for *Plasmodium falciparum* (24) interacting with *P. falciparum* Reticulocyte binding protein Homology 4 (PfRh4), and the interaction is crucial for invasion into erythrocytes (25–27). In addition, CR1 is also involved in the formation of rosettes by interacting with domains of *P. falciparum* Erythrocyte Membrane Protein 1 (PfEMP1) (28). Notably, in 2019, CR1 was shown to be involved in invasion by *P. vivax*, and the data showed that *P. vivax* invasion was reduced when the expression of CR1 level was low on erythrocytes and was inhibited by the addition of soluble CR1 (sCR1); however, this study showed that several PvRBP (orthologues of PfRh) proteins did not bind CR1 (29). Here, we have confirmed that sCR1 effectively blocked the binding of PvEBP-RII to erythrocytes. Furthermore, using ELISA, we verified that only one subdomain of CR1, Long Homology Repeat A (LHR-A), exhibited binding affinity for PvEBP-RII.

Results

Recombinant PvEBP-RII Binds to Both Normocytes and Reticulocytes Regardless of the Presence of DARC. The structure of PvEBP is similar to PvDBP with a signal peptide, a Duffy-binding-like domain (DBL), a cysteine-rich domain before a transmembrane domain, and a short cytosolic domain (Fig. 1A) (16). Because region II of PvDBP is able to bind to DARC-positive erythrocytes (3, 30), for further experiments, we expressed PvEBP-RII as a recombinant

protein in mammalian cells (Expi293 expression system) with rat CD4 domain 3 and 4 and histidine tag at C-term and purified it by nickel column and size exclusion chromatography. Three peaks were detected after size exclusion chromatography and the purified PvEBP-RII from each was resolved by SDS-PAGE which showed a single band at 62 kDa. The purified protein from P3 was used for further study (Fig. 1B and C). In our previous report, PvEBP-RII expressed on COS7 cells had binding activity to not only DARC-positive but also DARC-negative erythrocytes with a smaller size of the rosettes compared to PvDBP-RII in DARC-positive erythrocytes (14). To verify the previous findings, we evaluated the binding activity of the recombinant PvEBP-RII protein in both DARC-positive and -negative erythrocytes (Fig. 2). It is well known that *P. vivax* merozoites prefer young erythrocytes (reticulocytes) for invasion (31–33); hence, reticulocytes enriched from the buffy coat were used for further study. The level of DARC and CR1 on erythrocytes was measured by DARC and CR1 specific antibodies (Fig. 2A and B). As expected, PvEBP-RII bound to DARC-positive erythrocytes (Fig. 2C and See SI Appendix, Fig. S1). In addition, DARC-negative erythrocytes were also tested for the binding activity, and its binding was similar to that of DARC-positive erythrocytes (Fig. 2D and SI Appendix, Fig. S2). As a control, *P. vivax* Apical Membrane Antigen 1 (PvAMA1) and *P. falciparum* AMA1 (PfAMA1) recombinant proteins expressed similarly to PvEBP-RII were allowed to bind to DARC-positive and -negative erythrocytes. As expected, PvAMA1 but not PfAMA1, bound to DARC-positive and -negative erythrocytes (SI Appendix, Fig. S3) (34). These results demonstrate that PvEBP-RII binds both DARC-positive and -negative erythrocytes.

PvEBP-RII Binds to CR1. Invasion of *Plasmodium* merozoites relies on multiple interactions among merozoite ligands and their corresponding receptors on erythrocytes. It is therefore important to identify the proteins involved in this interaction to understand the molecular mechanism of invasion and develop new vaccines. Thus, we used the AVEXIS assay by which an interaction between *P. falciparum* RBP homology 5 (PfRh5) and Basigin was identified (18).

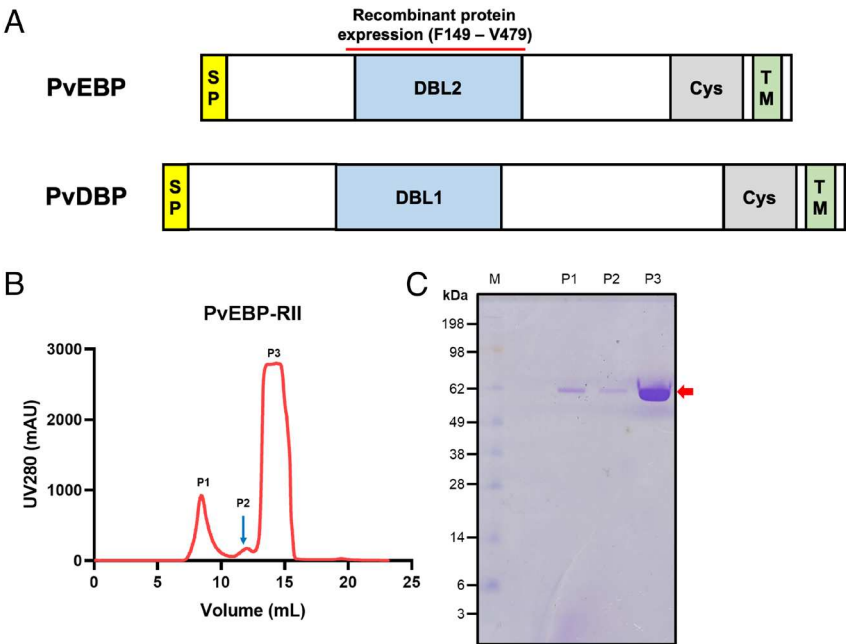


Fig. 1. Recombinant PvEBP-RII protein expression and purification. (A) Schematic structure of PvEBP and PvDBP. Both proteins have similar features; a signal peptide, a DARC binding-like (DBL) domain, a cysteine-rich domain (Cys), a transmembrane (TM), and a short cytosolic domain at the C terminus. Red bar represents the domain for recombinant protein expression (F149–V479). (B) Recombinant PvEBP-RII (~62 kDa with rat CD4 domains 3 and 4) was purified by size exclusion chromatography and (C) the protein in each peak was separated in a 4 to 12% SDS-PAGE and stained with Coomassie blue.

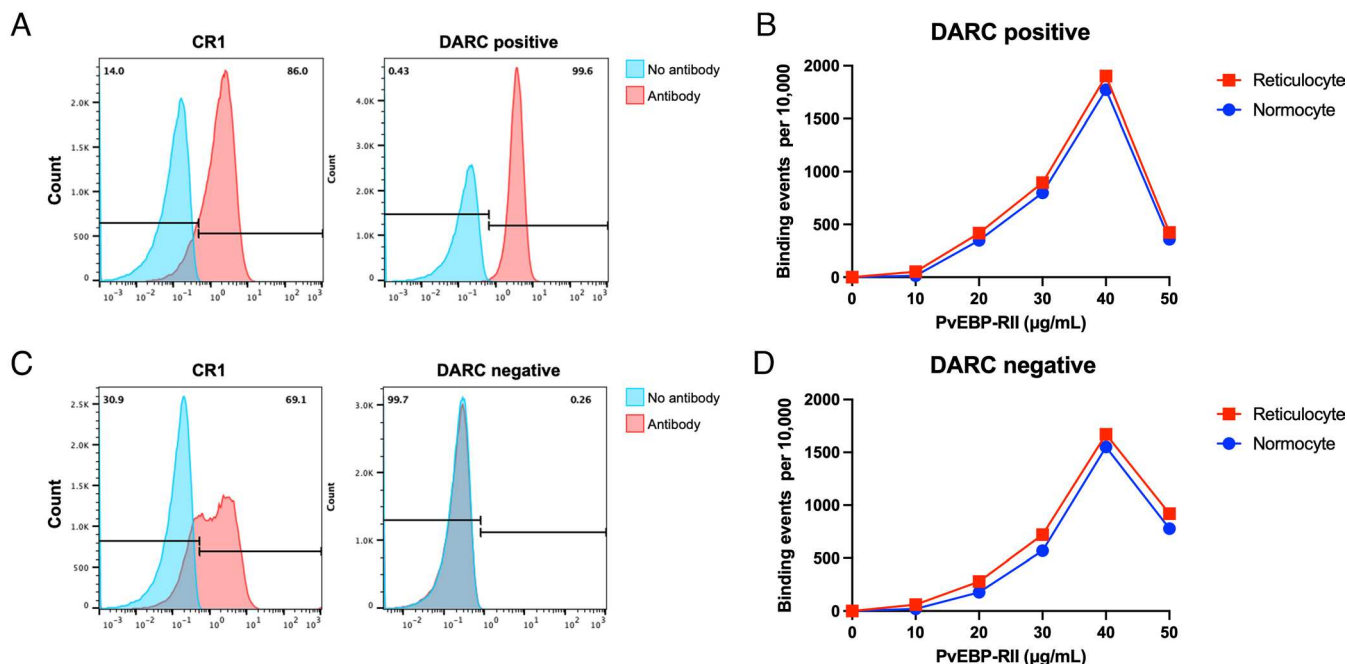


Fig. 2. PvEBP-RII binds to both reticulocytes and normocytes regardless of Duffy antigen receptor for chemokines (DARC). (A and B) DARC-positive and -negative erythrocytes and complement receptor 1 (CR1) were measured using mAbs against DARC and CR1, respectively, for each sample before the binding assay. Samples without Ab served as a negative control. (C and D) Varying concentrations of PvEBP-RII were incubated with reticulocyte-enriched erythrocytes in the presence (C) or absence (D) of DARC. The result represents a single experiment with four or three repeats for DARC-positive or -negative cells, respectively, and the others are shown in *SI Appendix, Figs. S1 and S2*.

A recombinant protein library containing over 750 human receptor ectodomains (18–21) was tested for a direct interaction with PvEBP-RII. Positive interactions for PvEBP-RII were observed with only three baits: CR1, CLC4M, and CEACAM1 (Fig. 3). The screening plate tested is shown in *SI Appendix, Fig. S4*. Both CLEC4M and CEACAM1 are lectins that interacted with many (>90) other preys (21), most likely by binding glycans present on these proteins. In the case of CR1, we observed binding to 27 other preys: one of them gave an extremely weak (“low confidence”) signal, while the other 26 had more complex binding profiles and interacted with the same set of seven receptors including CR1.

We concluded that these 26 other CR1 interactors were either misfolded parasite proteins that gave non-specific binding patterns or that bound to glycans present on this set of human receptors. In either case, the binding profile we observed for PvEBP was clearly distinct from the 26 other CR1-interacting proteins and we concluded that CR1 was a specific PvEBP-RII binding partner (Fig. 3 and *SI Appendix, Fig. S4*).

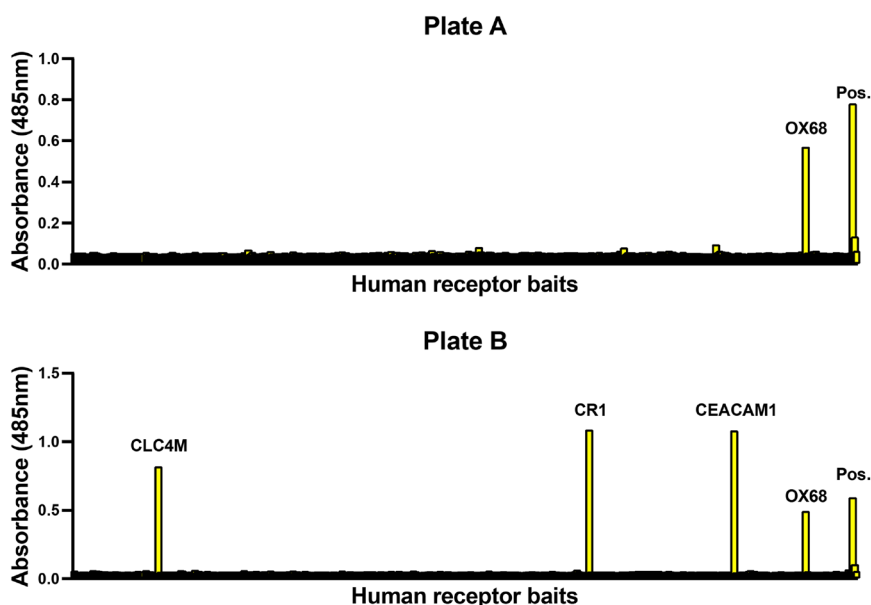


Fig. 3. AVEXIS demonstrates that PvEBP-RII interacts with CR1. A total of 754 human receptors were expressed as enzymatically monobiotinylated soluble ectodomain “baits” and captured on two 384-well streptavidin-coated microtiter plates. (Plate A and B) The receptor bait arrays were systematically tested for direct interactions with a PvEBP-RII “prey” formed by clustering biotinylated PvEBP-RII around a streptavidin-HRP conjugate. Two positive controls were present on each plate: “OX68” which represents an antibody that captures all prey and “Pos” which represents the rat Cd200-Cd200R interaction with Cd200 immobilized as the bait and Cd200R presented as the prey.

Additionally, we evaluated this interaction by ELISA (25, 35). The result revealed the binding of PvEBP-RII to plate-bound sCR1 in a dose-dependent manner, while the negative control protein (*Anopheles gambiae* D7L1) had no interaction (Fig. 4A). Furthermore, CR1 was present on both the DARC-positive and -negative erythrocytes (Fig. 2A and B) used for the binding assay and showed similar binding activities (Fig. 2C and D). Consequently, we demonstrated a specific interaction between CR1 and PvEBP-RII.

sCR1 Blocks the Binding of PvEBP-RII to Erythrocytes. Given that PvEBP-RII interacts with CR1 on erythrocytes, a binding inhibition assay was performed to assess whether sCR1 could block the binding of PvEBP-RII to erythrocytes. sCR1 was pre-incubated with PvEBP-RII before being added to erythrocytes. The results demonstrate that increasing concentrations of sCR1 led to a dose-dependent inhibition of PvEBP-RII binding to erythrocytes (in both DARC-positive and -negative erythrocytes). These results further establish that sCR1 is the receptor for PvEBP-RII (Fig. 4B and C and SI Appendix, Fig. S5).

LHR-A Interacts with PvEBP-RII. CR1 is divided into four equally sized and shaped subdomains called LHRs (35). Due to the substantial similarity between LHR-B and -C (~98%), LHR-C was not included in this experiment; thus, we expressed and purified recombinantly LHR-A, -B, and -D+ (SI Appendix, Fig. S6). To evaluate protein–protein interactions, ELISA methodology was

carried out, in which PvEBP-RII was biotinylated for detection (SI Appendix, Fig. S7A). A plate was coated with recombinant LHRs as well as negative control (*A. gambiae* D7L1) and incubated with the biotinylated PvEBP-RII. We observed that PvEBP-RII interacted with LHR-A in a dose-dependent manner but not with LHR-B or -D+ (Fig. 5A). The concentration of streptavidin-HRP used in Fig. 5A (1:10,000) is lower than that in Fig. 4A (1:5,000) where sCR1 bound PvEBP-RII because the higher concentration of streptavidin-HRP increased in OD value of LHR-A over 2. As a control, *A. gambiae* D7L1 (negative control) was biotinylated for detection along with PvEBP-RII (SI Appendix, Fig. S7A). In contrast to PvEBP-RII, we observed no interaction of *A. gambiae* D7L1 to the LHRs tested (SI Appendix, Fig. S7B and C). Hence, these results further indicate that LHR-A is the binding domain of PvEBP-RII (Fig. 5A and SI Appendix, Fig. S7B).

We also evaluated the inhibitory activity of LHRs for PvEBP-RII binding to erythrocytes. As shown in Fig. 5B, the recombinant LHR-A blocked the binding of PvEBP-RII to erythrocytes which is consistent with the ELISA-based binding assay result, whereas LHR-B and -D+ did not show inhibition.

Discussion

The absence of reliable methodologies for an in vitro *P. vivax* culture system has hampered studying the biology of this parasite and thereby, delaying the progress of efficient drugs and vaccines

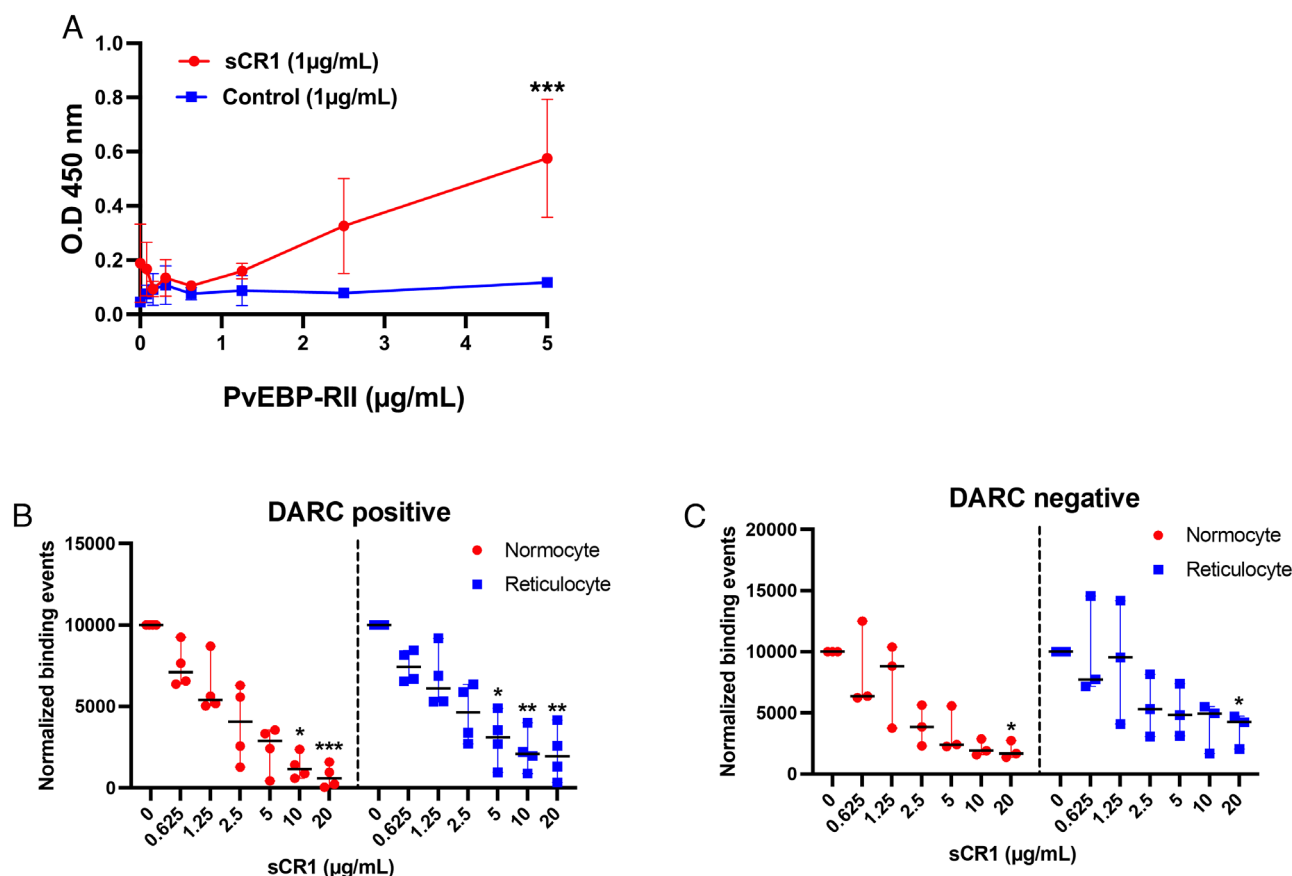


Fig. 4. sCR1 interacts with PvEBP-RII and blocks binding of PvEBP-RII to erythrocytes. (A) Microplates were coated with sCR1 or a negative control protein (*A. gambiae* D7L1—1 μg/mL) and incubated with varying concentrations of biotinylated PvEBP-RII. Streptavidin-HRP (1:5,000) was used to detect the bound protein. Displayed values are the means ±95% CI of three independent experiments. Statistical significance was determined by the unpaired *t* test, where $P < 0.05$ is considered significant (*** $P < 0.001$). (B and C) Serial dilutions of sCR1 (0 to 20 μg/mL) were co-incubated with PvEBP-RII protein (40 μg/mL) for 30 min at RT prior to incubation with erythrocytes to evaluate whether sCR1 inhibited the binding of PvEBP-RII to erythrocytes. After incubation, erythrocyte binding by PvEBP-RII was measured by flow cytometry. Data from four (B) or three (C) independent experiments were normalized to control (0 μg/mL). Values are median with the range. Statistical significance was determined by Friedman test, where $P < 0.05$ is considered significant (* $P < 0.05$; ** $P < 0.01$; *** $P < 0.001$).

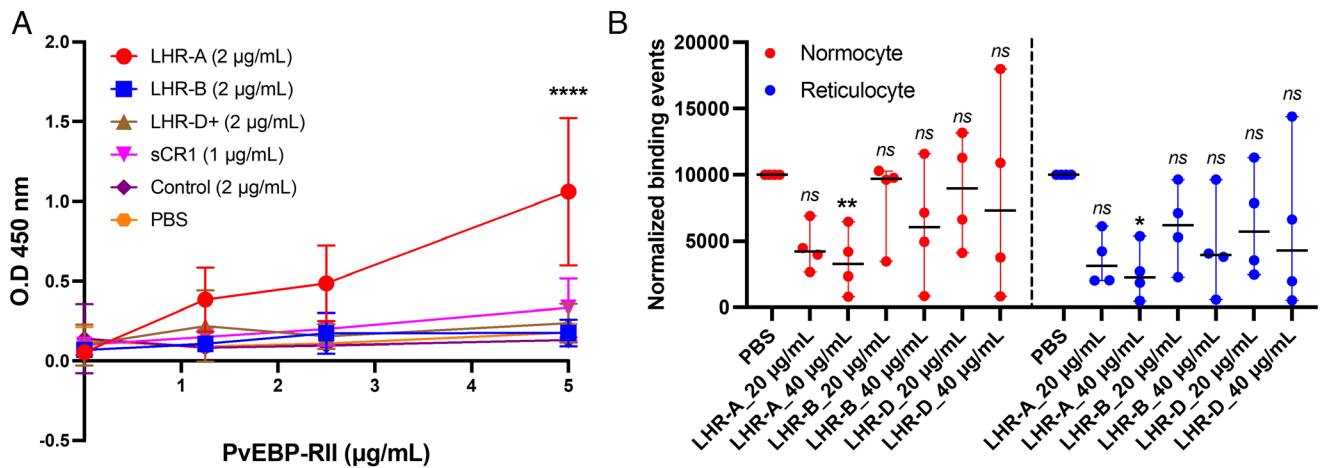


Fig. 5. Long homology region A (LHR-A) binds to PvEBP-RII and blocks binding of PvEBP-RII to erythrocytes. (A) Microplates were coated with LHRs (2 µg/mL), a negative control protein (*A. gambiae* D7L1—2 µg/mL), or sCR1 (1 µg/mL) and incubated with varying concentrations of biotinylated PvEBP-RII. Streptavidin-HRP (1:10,000) was used to detect the bound protein. Displayed values are the means \pm 95% CI of five independent experiments. Statistical significance was determined by a one-way ANOVA, where $P < 0.05$ is considered significant (**** $P < 0.0001$). (B) Two concentrations of LHRs (20 or 40 µg/mL) were co-incubated with PvEBP-RII protein (40 µg/mL) for 30 min at RT prior to incubation with DARC-positive erythrocytes to evaluate whether LHRs inhibited the binding of PvEBP-RII to erythrocytes. After incubation, erythrocyte binding by PvEBP-RII was measured by flow cytometry. Data from four independent experiments were normalized to control (PBS). Values are median with the range. Statistical significance was determined by Friedman test, where $P < 0.05$ is considered significant (* $P < 0.05$, ** $P < 0.01$) and *ns*: not significant.

specifically targeting this parasite. Although *P. vivax* belongs to the *Plasmodium* genus, it has distinct features such as *P. vivax* merozoites prefer reticulocytes for invasion unlike *P. falciparum* which invades erythrocytes of all ages. Hence, studies to discover the receptors of *P. vivax* merozoites have focused on reticulocyte-specific proteins, leading to the identification of some receptors such as transferrin receptor 1 (CD71) and SLC3A2 (CD98hc) which interact with PvRBP2b and PvRBP2a, respectively (5, 7). However, only a few host receptors for *P. vivax* have been identified compared to the number of parasite ligands that were confirmed binding to either or both reticulocytes and erythrocytes (36). This leads us to the evaluation of protein–protein interaction to discover the receptors for *P. vivax*.

AVEXIS is a method specifically designed to detect low-affinity extracellular protein interactions by clustering enzyme-tagged binding probes to increase binding avidity. Entire ectodomains of receptors are expressed as soluble recombinant proteins using a mammalian cell protein expression system to increase the chance that the proteins are correctly folded (19). Because of these features, the system has been used for studying protein–protein interactions in diverse fields, including host–parasite interactions and to identify Basigin on erythrocytes as a receptor for *P. falciparum* via interaction with the PFRh5 complex (18). Here, we have applied the AVEXIS system to identify CR1 as the receptor of PvEBP (Fig. 3). CR1, also known as the C3b/C4b receptor or CD35, is present on many different cell types including erythrocytes and interacts with complement components that opsonize antigens to clear them (37, 38). Moreover, CR1 is a recognized receptor for *P. falciparum* Rh4 that can compensate for the absence of *P. falciparum* Erythrocyte Binding Antigen-175 during invasion and is a vital receptor in the sialic acid-independent invasion pathway (26). In addition to *P. falciparum*, a previous study reported that sCR1 partially inhibited the invasion of *P. vivax* merozoites into reticulocytes, indicating the importance of CR1 for the parasite (29).

In our previous study, we observed that PvEBP ligand expressed on COS7 cells bound less strongly to human erythrocytes with smaller size of rosettes than PvDBP (14). This difference might be due to the fact that even though PvEBP and PvDBP have

similar structural features, especially the DBL domain (Fig. 1A), different amino acids with low identity in DBL (36%) and whole sequences (25%) could confer different properties (16). Indeed, we verified that PvEBP-RII bound erythrocytes independently of DARC. However, it remains to be solved why PvEBP-RII has lower binding activity for erythrocytes despite high level of CR1 compared to DARC on DARC-positive erythrocytes (Fig. 2A and C).

The binding of PvEBP-RII to both DARC-positive and -negative erythrocytes indicates that this protein may function as a ligand for parasite invasion in DARC-negative Africans. We assume that *P. vivax* merozoites may utilize both PvDBP and PvEBP for invasion into DARC-positive erythrocytes, whereas only PvEBP or/and another ligand allows invasion of DARC-negative erythrocytes. The difference in binding activity between PvDBP and PvEBP may account for the lower parasitemia observed in DARC-negative individuals infected with *P. vivax* (39, 40). Consequently, considering the emergence of *P. vivax* infections among DARC-negative Africans, the development of a vaccine together with PvEBP may be useful.

In conclusion, PvDBP is the leading vaccine candidate for the blood stage in *P. vivax* (41), but the high polymorphism and strain-specific immune response of PvDBP-RII may hinder the development of an efficient vaccine. Furthermore, the reporting of increasing *P. vivax* infection in DARC-negative populations raises the need for discovering additional ligands that are involved in both DARC-dependent and -independent erythrocyte invasion. PvEBP is one such candidate. The full list of host receptors and *P. vivax* ligands remains to be defined to understand the “full” invasion mechanisms. Most important is the development of a vaccine for children in Africa who suffer from *P. vivax* and have a problem with unrecognized infections that remain untreated and may lead to anemia (42). As we look to the future, *P. vivax* must be in our sights for vaccines for African children who are DARC-negative. Recently, two studies have shown that a subpopulation of red blood cell progenitor is expressing low level of DARC and was invaded by *P. vivax* (43–45). However, it is still unknown whether DARC is a receptor for *P. vivax* infection of DARC-negative people in Africa or whether PvDBP-RII can be

a vaccine for DARC-negative people. Alternatively, other *P. vivax* ligands such as PvEBP and PvRBP2, may be used for vaccines. For both *P. falciparum* (25, 26) and *P. vivax*, the interaction with CR1 receptors predominantly occurs in the first subdomain, LHR-A of CR1. Could this indicate that the LHR-A of CR1 is more accessible for binding by parasite ligands? While the precise structure of CR1 on erythrocytes remains elusive, these studies offer valuable insights that could contribute to a deeper understanding of its function and interaction with parasite ligands.

Materials and Methods

Recombinant Protein Expression and Purification. The gene fragment encoding PvEBP-R11 (Phe179 – Val479) (PlasmidDB: PVP01_0102300) after codon-optimization with point mutation at a predicted N-glycosylation site (T443A) was synthesized by GenScript in a pcDNA3.3 vector for a mammalian cell expression. The synthesized gene was digested by *Ascl* and *NotI* restriction enzymes (New England Lab, NEB) and inserted into BMR1_01g020310-bio-His (Addgene plasmid # 108116) (Addgene) which contains rat CD4 domain 3 and 4 and histidine tag at C-term (~25 kDa) with T4 DNA ligase (NEB). Dideoxynucleotide DNA sequencing on an ABI (Applied Biosystems) 3730XL 96-capillary sequencer was employed to confirm all the constructed plasmids. The constructs harboring PvEBP-R11, LHR-A (CCP1-7), -B (CCP8-14), and -D+(CCP22-30) (25, 35, 46–50) were transfected into human embryonic kidney cells, Expi293 (American Type Culture Collection), and incubated at 37 °C for recombinant protein expression. Seventy-two hours after transfection, culture supernatants were harvested and processed for protein purification. The transfection and protein expression were performed at the Leidos Biomedical Research, Inc.

The recombinant proteins were purified as described in a previous report (34) using affinity chromatography with Nickel-charged HiTrap Chelating HP or HisTrap excel (Cytiva) followed by size-exclusion chromatography with Superdex 200 10/300 GL columns (Cytiva) according to the manufacturer's instructions. The protein purification with the column was carried out with the AKTA purifier system (GE Healthcare Life Science). The purified proteins were assessed on an SDS-PAGE (NuPAGE Novex 4–12% Bis-Tris protein gels, Thermo Fisher Scientific) under denaturing conditions. To visualize the proteins, the gels were stained with Coomassie blue by the eStain protein stain system (GenScript).

Human Receptor Interaction Screening. A recombinant protein library containing 754 human receptor ectodomains was expressed as soluble "bait" proteins in HEK293E cells from plasmids described in previous studies (18, 20, 21, 51). HEK293E cells were co-transfected with a plasmid encoding a secreted BirA enzyme (52) which enzymatically biotinylated a biotin acceptor site to produce soluble monobiotinylated ectodomains. Spent supernatants were centrifuged at 2,000 g for 20 min, filtered through 0.22 µm filters, and purified by nickel-ion affinity chromatography using His MultiTrap plates (GE Healthcare) and a 96-position pneumatic press (53). Before purification, each supernatant was supplemented with 16 mM imidazole and 200 mM NaCl. The plates were washed with 500 µL of water, followed by 500 µL of 30 mM imidazole phosphate buffer following the manufacturer's instructions. After all samples were loaded, plates were washed twice with 500 µL of 30 mM imidazole phosphate buffer and eluted with 200 µL of 400 mM imidazole phosphate buffer. Protein concentrations were measured using a Bradford Assay, and integrity was checked by SDS-PAGE as described (21). Streptavidin-coated 384-well screening plates (Greiner) were prepared by washing in 80 µL HEPES-Buffered Saline (HBS) with 0.1% Tween-20 (HBS-T), and blocked in 2% BSA in HBS (10 mM HEPES, 1 mM MgCl₂, 2 mM CaCl₂, 5 mM KCl, 140 mM NaCl, pH 7.4) for more than 30 min at 20 °C. Purified human receptor bait proteins were diluted in 2% BSA in HBS so that each 50 µL well would contain 100 femtomoles of biotinylated protein for arraying using a Hamilton microlab star fluid handling robot. After bait immobilization, plates were washed three times in 50 µL HBS-T supplemented with 0.8 µM desthiobiotin (Sigma) to block any vacant biotin-binding sites.

The PvEBP-R11 was expressed together with a CD4d3+4 tag (25 kDa) resulting in a recombinant protein of 62 kDa and purified as described above. Purified soluble biotinylated PvEBP-R11 protein was clustered around 6.25 fmol streptavidin-HRP (Pierce) with the calculated stoichiometric equivalent of 25 fmol recombinant

protein for 30 min at 20 °C to form a "prey." Clustered PvEBP was then diluted to 20-fold in 2% BSA in HBS before applying 50 µL per well for 1 h at 20 °C, washed twice using 75 µL of desthiobiotin in HBS-T, followed by a final wash in 75 µL of HBS. Immediately after, 30 µL of TMB chromogenic substrate (Millipore) was added and incubated at 20 °C for 20 min. The reaction was stopped by adding 30 µL of 0.3% NaF (Sigma). Plates were measured on a Tecan Spark plate reader at absorbance at 650 nm as described (21).

Reticulocyte Enrichment from Buffy Coat. Buffy coats from DARC-positive or -negative individuals were used for reticulocyte enrichment (The Blood Bank, NIH) according to previous reports (34, 54). Briefly, leukocytes were removed through a Non-Woven Fabric (NWF) filter (Zhixing Bio Co.), and purified erythrocytes were suspended at a 20% hematocrit in high-KCl buffer [115 mM KCl, 20 mM N-2-hydroxyethylpiperazine-N-2-ethane sulfonic acid (HEPES), 1 mM NaH₂PO₄, 1 mM MgCl₂, 0.5 mM ethylenediaminetetraacetic acid (EDTA), 10 mM D-glucose, and 12 mM NaCl, pH 7.4]. The diluted erythrocytes were overlaid on 19% Nycodenz (w/v) from a 60% Nycodenz stock (w/v), which is dissolved in water (Axis-Shield PoC), in high-KCl buffer and spun down at 3,000 g for 30 min without a brake. The enriched reticulocytes in interlayer were collected and washed three times with incomplete Roswell Park Memorial Institute (RPMI) 1640 medium [containing 2 mM L-glutamine, 25 mM HEPES, and 5 mg/L hypoxanthine (KD Medical Inc.)]. The enriched reticulocytes were stained by new methylene blue for 15 min and evaluated in thin blood smear (55).

Erythrocyte Binding Assay and Binding Inhibition Assay. Erythrocyte binding assay and inhibition assay were carried out as described in a previous report (34). Briefly, reticulocyte-enriched erythrocytes prepared as described above were incubated with recombinant PvEBP-R11 protein for 3 h at room temperature (RT). For the binding inhibition assay, the PvEBP-R11 protein was pre-incubated with either sCR1 or LHRs prior to incubation with erythrocytes. The erythrocytes were incubated with Alexa Fluor 647-conjugated mouse anti-His monoclonal antibody (QIAGEN) and the reticulocytes were stained with the Thiazole Orange Retic-COUNT reagent (TO) (Becton Dickinson) before analysis. A total of 100,000 events per sample were analyzed with MACSQuant® Analyzer 10 (Miltenyi Biotec), and resulting data were analyzed with FlowJo 10. 8. 1 (FlowJo LLC). Unstained cells and TO-stained cells were used to separate the normocytes and reticulocytes, respectively. The following formula was used to calculate the binding events of PvEBP-R11 to normocytes and reticulocytes (Fig. 2 C and D and *SI Appendix, Figs. S1 and S2*): Binding events = Binding cells/Total cells (Binding cells + Unbound cells). Binding cells for normocyte and reticulocyte are represented in Q1 and Q2, respectively. Unbound cells for normocytes and reticulocytes are represented in Q4 and Q3, respectively. Binding events were calculated for each control (0 µg/mL) that is fixed to be 10,000 events (Figs. 4 B and C and 5B) to normalize binding inhibition data. The number of binding events of PBS samples was subtracted from each sample of the experiments.

Biotinylation of PvEBP-R11. Recombinant PvEBP-R11 and *A. gambiae* D7L1 were biotinylated by EZ-Link™ Micro Sulfo-NHS-Biotinylation kit (Thermo Fisher Scientific) according to the manufacturer's instructions. Briefly, the proteins were incubated with the appropriate volume of Sulfo-NHS-Biotin solution at RT for 30 min, and the reaction was eluted through Zeba Spin Desalting Column by centrifugation. The biotinylated proteins were evaluated by Pierce™ Biotin Quantitation Kit (Thermo Fisher Scientific).

ELISA to Evaluate Protein-Protein Interactions. ELISA was carried out to evaluate protein-protein interaction following as described before (35) with minor modifications. Briefly, 96-well microplates (Corning®) were coated with LHR-A, -B, -D+, sCR1 (predicted molecular weight is 213 kDa) (R&D Systems), or negative control (*A. gambiae* D7L1, 35 kDa) at 4 °C overnight. The coated wells were blocked with 1% BSA in PBS at 37 °C for 2 h and incubated with biotinylated PvEBP-R11 at varying concentrations in PBS with 0.05% Tween-20 at RT for 2 h. The bound protein was detected by incubation with Horseradish peroxidase (HRP)-Conjugated Streptavidin (1:5,000 or 1:10,000 for Figs. 4A or 5A, respectively) (Thermo Fisher Scientific) in 1% BSA in PBS at RT for 1 h. The plate was washed with PBS three times after each step. 1-Step™ TMB ELISA Substrate Solutions (Thermo Fisher Scientific) was used to detect HRP activity. The reaction was stopped by addition of ELISA Stop Solution (Invitrogen™, Thermo Fisher

Scientific) after 30 min, and optical density was measured at 450 nm by GloMax® Explorer Multimode Microplate Reader (Promega).

Statistical Analysis. All data were statistically analyzed and plotted using GraphPad Prism 10. For the ELISA analysis, at least three independent experiments were performed for each condition and the number of the repeats was indicated in figure legends. For the erythrocyte binding assay, resulting event data from cytometric analyses were recalculated against the respective controls used in each experiment (0 µg/mL added component) and normalized to 10,000 events. The resulting event data points were multiplied with the same factor to overcome inherent data variability between experimental repeats. The data relation between data groups was not altered by these steps, nonetheless improved comparability. As the rescaled data confirmed approximately with underlying assumptions for non-parametric testing, Friedman test was generally applied. Graphs show the data median with range.

Data, Materials, and Software Availability. All study data are included in the article and/or *SI Appendix*.

ACKNOWLEDGMENTS. This work was supported by the Intramural Research Program of the Division of Intramural Research, National Institute of Allergy and Infectious Diseases, NIH. Dr. G.J.W. and Dr. C.C. were supported by the Wellcome Trust (grant 206194). We thank Dr. Susan K. Pierce, NIH for valuable suggestions, Johannes S. P. Doehl for statistical analysis, and Caroline Percopo for the help in Flow Cytometry. We thank Hyon Ju Park, M. Kathryn Liszewski, Richard Hauhart, Malgorzata Krych, Dennis Hourcade, Liliana Clemenza, and Bala Subramanian for their pioneering studies on CR1 including characterization of CR1 allotypes utilized in this study.

Author affiliations: ^aLaboratory of Malaria and Vector Research, National Institute of Allergy and Infectious Diseases, NIH, Rockville, MD 20852; ^bDepartment of Biology, Hull York Medical School, York Biomedical Research Institute, University of York, York YO10 5DD, United Kingdom; ^cLaboratory of Immunogenetics, National Institute of Allergy and Infectious Diseases, NIH, Rockville, MD 20852; ^dRheumatology Fellowship Training Program, National Institute of Arthritis and Musculoskeletal and Skin Diseases, Bethesda, MD 20892; and ^eDivision of Rheumatology, Department of Medicine, Washington University School of Medicine, Saint Louis, MO 63110

1. R. E. Howes *et al.*, Global epidemiology of *Plasmodium vivax*. *Am. J. Trop. Med. Hyg.* **95**, 15–34 (2016).
2. L. H. Miller, S. J. Mason, D. F. Clyde, M. H. McGinniss, The resistance factor to *Plasmodium vivax* in blacks. The Duffy-blood-group genotype, FyFy. *N. Engl. J. Med.* **295**, 302–304 (1976).
3. C. E. Chitnis, L. H. Miller, Identification of the erythrocyte binding domains of *Plasmodium vivax* and *Plasmodium knowlesi* proteins involved in erythrocyte invasion. *J. Exp. Med.* **180**, 497–506 (1994).
4. K. Gunalan, A. Nangaly, M. A. Thera, O. K. Doumbo, L. H. Miller, *Plasmodium vivax* infections of duffy-negative erythrocytes: Historically undetected or a recent adaptation? *Trends Parasitol.* **34**, 420–429 (2018).
5. J. Gruszczyk *et al.*, Transferrin receptor 1 is a reticulocyte-specific receptor for *Plasmodium vivax*. *Science* **359**, 48–55 (2018).
6. J. Gruszczyk *et al.*, Cryo-EM structure of an essential *Plasmodium vivax* invasion complex. *Nature* **559**, 135–139 (2018).
7. B. Malleret *et al.*, *Plasmodium vivax* binds host CD98hc (SLC3A2) to enter immature red blood cells. *Nat. Microbiol.* **6**, 991–999 (2021).
8. J. H. Han *et al.*, *Plasmodium vivax* Merozoite surface protein 1 paralog as a mediator of parasite adherence to reticulocytes. *Infect. Immun.* **86**, e00239–18 (2018).
9. Y. Cheng *et al.*, The *Plasmodium vivax* merozoite surface protein 1 paralog is a novel erythrocyte-binding ligand of *P. vivax*. *Infect. Immun.* **81**, 1585–1595 (2013).
10. Y. Cheng *et al.*, *Plasmodium vivax* GPI-anchored micronemal antigen (PvGAMA) binds human erythrocytes independent of Duffy antigen status. *Sci. Rep.* **6**, 35581 (2016).
11. J. Lu *et al.*, Glycosylphosphatidylinositol-anchored micronemal antigen (GAMA) interacts with the band 3 receptor to promote erythrocyte invasion by malaria parasites. *J. Biol. Chem.* **298**, 101765 (2022).
12. L. A. Baquero *et al.*, PvGAMA reticulocyte binding activity: Predicting conserved functional regions by natural selection analysis. *Parasit. Vectors* **10**, 251 (2017).
13. M. S. Alam *et al.*, Interaction of *Plasmodium vivax* tryptophan-rich antigen PvTRAg38 with Band 3 on human erythrocyte surface facilitates parasite growth. *J. Biol. Chem.* **290**, 20257–20272 (2015).
14. K. Gunalan *et al.*, Role of *Plasmodium vivax* duffy-binding protein 1 in invasion of duffy-null africans. *Proc. Natl. Acad. Sci. U.S.A.* **113**, 6271–6276 (2016).
15. F. B. Ntunmgia *et al.*, A novel erythrocyte binding protein of *Plasmodium vivax* suggests an alternate invasion pathway into duffy-positive reticulocytes. *mBio* **7**, e01261–16 (2016).
16. J. Hester *et al.*, De novo assembly of a field isolate genome reveals novel *Plasmodium vivax* erythrocyte invasion genes. *PLoS Negl. Trop. Dis.* **7**, e2569 (2013).
17. C. Roesch *et al.*, Genetic diversity in two *Plasmodium vivax* protein ligands for reticulocyte invasion. *PLoS Negl. Trop. Dis.* **12**, e0006555 (2018).
18. C. Crosnier *et al.*, Basigin is a receptor essential for erythrocyte invasion by *Plasmodium falciparum*. *Nature* **480**, 534–537 (2011).
19. S. J. Bartholdson, C. Crosnier, L. Y. Bustamante, J. C. Rayner, G. J. Wright, Identifying novel *Plasmodium falciparum* erythrocyte invasion receptors using systematic extracellular protein interaction screens. *Cell Microbiol.* **15**, 1304–1312 (2013).
20. Y. Sun *et al.*, A human platelet receptor protein microarray identifies the high affinity immunoglobulin E receptor subunit alpha (FcεpsilonR1alpha) as an activating platelet endothelium aggregation receptor 1 (PEAR1) ligand. *Mol. Cell Proteom.* **14**, 1265–1274 (2015).
21. J. Shilts *et al.*, A physical wiring diagram for the human immune system. *Nature* **608**, 397–404 (2022).
22. J. M. Moulds, M. W. Nickells, J. J. Moulds, M. C. Brown, J. P. Atkinson, The C3b/C4b receptor is recognized by the Knops, McCoy, Swain-langley, and York blood group antisera. *J. Exp. Med.* **173**, 1159–1163 (1991).
23. N. Rao, D. J. Ferguson, S. F. Lee, M. J. Telen, Identification of human erythrocyte blood group antigens on the C3b/C4b receptor. *J. Immunol.* **146**, 3502–3507 (1991).
24. C. Spadafora *et al.*, Complement receptor 1 is a sialic acid-independent erythrocyte receptor of *Plasmodium falciparum*. *PLoS Pathog.* **6**, e1000968 (2010).
25. W. H. Tham *et al.*, *Plasmodium falciparum* uses a key functional site in complement receptor type-1 for invasion of human erythrocytes. *Blood* **118**, 1923–1933 (2011).
26. W. H. Tham *et al.*, Complement receptor 1 is the host erythrocyte receptor for *Plasmodium falciparum* PfRh4 invasion ligand. *Proc. Natl. Acad. Sci. U.S.A.* **107**, 17327–17332 (2010).
27. N. T. Lim *et al.*, Characterization of inhibitors and monoclonal antibodies that modulate the interaction between *Plasmodium falciparum* adhesin PfRh4 with its erythrocyte receptor complement receptor 1. *J. Biol. Chem.* **290**, 25307–25321 (2015).
28. J. A. Rowe, J. M. Moulds, C. I. Newbold, L. H. Miller, *P. falciparum* rosetting mediated by a parasite-variant erythrocyte membrane protein and complement-receptor 1. *Nature* **388**, 292–295 (1997).
29. S. K. Prajapati *et al.*, Complement Receptor 1 availability on red blood cell surface modulates *Plasmodium vivax* invasion of human reticulocytes. *Sci. Rep.* **9**, 8943 (2019).
30. S. P. Wertheimer, J. W. Barnwell, *Plasmodium vivax* interaction with the human Duffy blood group glycoprotein: Identification of a parasite receptor-like protein. *Exp. Parasitol.* **69**, 340–350 (1989).
31. B. Mons, J. J. Croon, W. van der Star, H. J. van der Kaay, Erythrocytic schizogony and invasion of *Plasmodium vivax* in vitro. *Int. J. Parasitol.* **18**, 307–311 (1988).
32. C. Lim *et al.*, Reticulocyte preference and stage development of *Plasmodium vivax* isolates. *J. Infect. Dis.* **214**, 1081–1084 (2016).
33. B. Malleret *et al.*, *Plasmodium vivax*: Restricted tropism and rapid remodeling of CD71-positive reticulocytes. *Blood* **125**, 1314–1324 (2015).
34. S. K. Lee *et al.*, The direct binding of *Plasmodium vivax* AMA1 to erythrocytes defines a RON2-independent invasion pathway. *Proc. Natl. Acad. Sci. U.S.A.* **120**, e2215003120 (2023).
35. H. J. Park *et al.*, Using mutagenesis and structural biology to map the binding site for the *Plasmodium falciparum* merozoite protein PfRh4 on the human immune adherence receptor. *J. Biol. Chem.* **289**, 450–463 (2014).
36. J. Popovici, C. Roesch, V. Rougeron, The enigmatic mechanisms by which *Plasmodium vivax* infects Duffy-negative individuals. *PLoS Pathog.* **16**, e1008258 (2020).
37. M. J. Boyle *et al.*, Human antibodies fix complement to inhibit *Plasmodium falciparum* invasion of erythrocytes and are associated with protection against malaria. *Immunity* **42**, 580–590 (2015).
38. S. Biryukov *et al.*, Complement and antibody-mediated enhancement of red blood cell invasion and growth of malaria parasites. *EBioMedicine* **9**, 207–216 (2016).
39. E. Lo *et al.*, Contrasting epidemiology and genetic variation of *Plasmodium vivax* infecting Duffy-negative individuals across Africa. *Int. J. Infect. Dis.* **108**, 63–71 (2021).
40. A. Nangaly *et al.*, *Plasmodium vivax* infections over 3 years in Duffy blood group negative malians in Bandiagara, Mali. *Am. J. Trop. Med. Hyg.* **97**, 744–752 (2017).
41. S. Kar, A. Sinha, *Plasmodium vivax* Duffy binding protein-based vaccine: A distant dream. *Front. Cell Infect. Microbiol.* **12**, 916702 (2022).
42. N. M. Douglas *et al.*, The anaemia of *Plasmodium vivax* malaria. *Malar J.* **11**, 135 (2012).
43. I. Bouyssou *et al.*, Unveiling *P. vivax* invasion pathways in Duffy-negative individuals. *Cell Host Microbe*, 10.1016/j.chom.2023.11.007 (2023).
44. C. Dechavanne *et al.*, Duffy antigen is expressed during erythropoiesis in Duffy-negative individuals. *Cell Host Microbe* **31**, 2080–2092.e5 (2023), 10.1016/j.chom.2023.10.019.
45. P. E. Duffy, K. Gunalan, L. H. Miller, *Vivax* malaria and Duffy antigen: Stop being so negative. *Cell Host Microbe* **31**, P1959–P1960 (2023).
46. M. Krych, D. Hourcade, J. P. Atkinson, Sites within the complement C3b/C4b receptor important for the specificity of ligand binding. *Proc. Natl. Acad. Sci. U.S.A.* **88**, 4353–4357 (1991).
47. M. Krych *et al.*, Analysis of the functional domains of complement receptor type 1 (C3b/C4b receptor; CD35) by substitution mutagenesis. *J. Biol. Chem.* **269**, 13273–13278 (1994).
48. V. B. Subramanian, L. Clemenza, M. Krych, J. P. Atkinson, Substitution of two amino acids confers C3b binding to the C4b binding site of CR1 (CD35). Analysis based on ligand binding by chimpanzee erythrocyte complement receptor. *J. Immunol.* **157**, 1242–1247 (1996).
49. M. Krych, R. Hauhart, J. P. Atkinson, Structure-function analysis of the active sites of complement receptor type 1. *J. Biol. Chem.* **273**, 8623–8629 (1998).
50. M. Krych-Goldberg *et al.*, Decay accelerating activity of complement receptor type 1 (CD35). Two active sites are required for dissociating C5 convertases. *J. Biol. Chem.* **274**, 31160–31168 (1999).
51. K. Dundas *et al.*, Alpha-v-containing integrins are host receptors for the *Plasmodium falciparum* sporozoite surface protein, TRAP. *Proc. Natl. Acad. Sci. U.S.A.* **115**, 4477–4482 (2018).
52. J. S. Kerr, G. J. Wright, Avidity-based extracellular interaction screening (AVEXIS) for the scalable detection of low-affinity extracellular receptor–ligand interactions. *J. Vis. Exp.* **61**, e3881 (2012), 10.3791/3881.
53. Y. Sun, M. Gallagher-Jones, C. Barker, G. J. Wright, A benchmarked protein microarray-based platform for the identification of novel low-affinity extracellular protein interactions. *Anal. Biochem.* **424**, 45–53 (2012).
54. W. Roobsoong *et al.*, Improvement of culture conditions for long-term in vitro culture of *Plasmodium vivax*. *Malar J.* **14**, 297 (2015).
55. G. Brecher, New methylene blue as a reticulocyte stain. *Am. J. Clin. Pathol.* **19**, 895 (1949).